

SCIENTIFIC REPORTS



OPEN

Transferring arbitrary d -dimensional quantum states of a superconducting transmon qudit in circuit QED

Tong Liu¹, Qi-Ping Su¹, Jin-Hu Yang¹, Yu Zhang¹, Shao-Jie Xiong², Jin-Ming Liu² & Chui-Ping Yang¹ 

A qudit (d -level quantum system) has a large Hilbert space and thus can be used to achieve many quantum information and communication tasks. Here, we propose a method to transfer arbitrary d -dimensional quantum states (known or unknown) between two superconducting transmon qudits coupled to a single cavity. The state transfer can be performed by employing resonant interactions only. In addition, quantum states can be deterministically transferred without measurement. Numerical simulations show that high-fidelity transfer of quantum states between two superconducting transmon qudits ($d \leq 5$) is feasible with current circuit QED technology. This proposal is quite general and can be applied to accomplish the same task with natural or artificial atoms of a ladder-type level structure coupled to a cavity or resonator.

Many quantum information and communication tasks are usually based on qubits (two-level quantum systems), but the use of qudits (d -level quantum systems) can optimize some quantum computations^{1,2}, enhance the security of quantum cryptography^{3,4}, realize bipartite entanglement⁵, verify entropic inequalities⁶, implement quantum algorithms⁷, and simplify the construction of quantum logic gates^{8,9}. In addition, manipulation and measurement of a superconducting phase qudit state or preparation and control of a transmon qudit has been reported in experiments^{10,11}. Moreover, population transfer of a three-level transmon qudit for $d=3$, via stimulated Raman adiabatic passage, has been experimentally demonstrated recently¹².

During the past years, superconducting qubits/qudits have been paid intensive attention in quantum information and quantum computation due to their significantly increased coherence times, controllability and scalability^{13–21}. Superconducting qubits/qudits based on Josephson junctions are mesoscopic element circuits that behave like “artificial atoms”, whose level spacings can be rapidly (within 1–3 ns) adjusted by varying external control parameters (e.g., magnetic flux applied to the superconducting loop of a superconducting phase, transmon, Xmon, or flux qubit/qudit; see, e.g., refs 18, 22–24).

Circuit quantum electrodynamics (circuit QED) is analogue of cavity QED, which has been considered as one of the most promising candidates for quantum information processing (QIP)^{14, 15, 25–27}. The strong-coupling or ultrastrong-coupling regime with a superconducting qubit coupled to a microwave resonator has been experimentally realized in circuit QED^{28–31}. Using superconducting qubits coupled to a single cavity or resonator, many theoretical proposals have been presented for realizing quantum gates and entanglement^{25–27, 32–37}. Quantum effects and operations have been experimentally demonstrated with superconducting qubits in circuit QED, including demonstration of two- and three-qubit quantum gates^{38–42}, realization of two- and three-qubit entanglement^{23, 43}, observation of Raman coherence effects⁴⁴, and suppression of dephasing by qubit motion⁴⁵. Moreover, a number of theoretical proposals have been proposed for realizing quantum state transfer (QST) between two superconducting qubits through a cavity^{26, 33, 46–51}. The QST between two superconducting qubits has been experimentally demonstrated in circuit QED^{52–55}.

The qudit-to-qudit QST plays a vital role in high-dimensional quantum communication and QIP. Transfer of high-dimensional photon states through a cavity array was previously proposed in refs 56 and 57. In addition,

¹Department of Physics, Hangzhou Normal University, Hangzhou, Zhejiang, 310036, China. ²State Key Laboratory of Precision Spectroscopy, Department of Physics, East China Normal University, Shanghai, 200062, China. Correspondence and requests for materials should be addressed to C.-P.Y. (email: yangcp@hznu.edu.cn)



Figure 1. (a) Setup for two superconducting transmon qubits embedded in a 3D cavity. (b) Setup for two superconducting transmon qubits coupled to a 1D transmission line resonator. A dark dot represents a superconducting transmon qubit.

probabilistic transfer of high-dimensional quantum states between particles via a spin chain has been studied^{58,59}. Moreover, a method has been proposed for transferring quantum states between two superconducting transmon qubits via an adjustable inductive coupling⁶⁰, and an approach has been presented for transferring quantum states between two superconducting flux qutrits coupled to two resonators or cavities⁶¹. Here, qutrit refer to a three-level quantum system or a qudit for $d = 3$. Refs 60 and 61 only work for QST between two qutrits and ref. 61 requires the use of *two* resonators or cavities coupled to each qutrit. Note that in a circuit consisting of two or more resonators, the inter-resonator crosstalk is inevitable⁶², which degrades the performance of quantum operations and the fidelity of various quantum states.

Different from the previous works, we here propose a method to transfer arbitrary d -dimensional quantum states (known or unknown) between two superconducting transmon qubits coupled to a single cavity. As shown below, this proposal has the following advantages: (i) The experimental setup is very simple because only one cavity is used; (ii) Since employing a single cavity, the inter-cavity crosstalk is avoided; (iii) The QST can be realized by using qudit-cavity and qudit-pulse resonant interactions only; (iv) The QST can be deterministically achieved without measurement; and (v) The method can in principle be applied to transfer arbitrary d -dimensional quantum states between two d -level qubits for any positive integer d . This proposal is quite general and can be applied to accomplish the same task with “ladder-type level structure” natural or artificial atoms coupled to a cavity or resonator.

In this work, we will show how to transfer arbitrary quantum states between two superconducting transmon qubits coupled to a cavity or resonator. We will also discuss the experimental feasibility of this proposal, by considering a setup of two transmon qubits coupled to a 3D cavity and numerically calculating the fidelity for the QST between two transmon qubits for $d \leq 5$.

Results

Quantum state transfer between two superconducting transmon qubits. Our system, shown in Fig. 1, consists of two superconducting transmon qubits 1 and 2 embedded in a 3D microwave cavity or coupled to a 1D resonator. In reality, the d involved in QIP may not be a large number. Thus, as an example, we will explicitly show how to transfer quantum states between two transmon qubits for $d \leq 5$. We then give a brief discussion on how to extend the method to transfer arbitrary d -dimensional quantum states between two d -level transmon qubits for any positive integer d .

A transmon qubit has a ladder-type level structure⁶³. We here label the d levels as $|0\rangle$, $|1\rangle$, $|2\rangle$, ... and $|d-1\rangle$ (Fig. 2 for $d=5$). For a ladder-type level structure, the transition between adjacent levels is allowed but the transition between non-adjacent levels is forbidden or very weak. In the following, the transition frequency between two adjacent levels $|l-1\rangle$ and $|l\rangle$ of each qudit is labeled as $\omega_{(l-1)l}$ ($l=1, 2, \dots, d-1$). The initial phase, duration, and frequency of the pulses are denoted as $\{\phi, t, \omega\}$. For simplicity, we set the same Rabi frequency Ω for each pulse, which can be readily achieved by adjusting the pulse intensity. Here and below, qudit (qudits) refers to transmon qudit (qudits).

Case for $d=5$. The five levels of qubits are labeled as $|0\rangle$, $|1\rangle$, $|2\rangle$, $|3\rangle$, and $|4\rangle$ (Fig. 2). Assume that qudit 1 is initially in an arbitrary quantum state $\sum_{l=0}^4 c_l |l\rangle_1$ (known or unknown) with level populations illustrated in Fig. 2(a), qudit 2 is initially in the ground state $|0\rangle_2$, and the cavity is initially in the vacuum state $|0\rangle_c$. Here and below, c_l is a normalized coefficient.

To begin with, the level spacings of the qubits need to be adjusted to have the cavity resonant with the $|0\rangle \leftrightarrow |1\rangle$ transition of each qudit. The procedure for implementing the QST from qudit 1 to qudit 2 is described as follows:

Step I. Let the cavity resonant with the $|0\rangle \leftrightarrow |1\rangle$ transition of each qudit described by Hamiltonian (14) (see Section Methods below). According to Eq. (15), after an interaction time $t_1 = \pi/(\sqrt{2}g)$, one has the state transformation

$$|1\rangle_1 |0\rangle_c |0\rangle_2 \rightarrow -|0\rangle_1 |0\rangle_c |1\rangle_2, \quad (1)$$

which shows that the cavity remains in the vacuum state after the qudit-cavity interaction. Thus, the initial state $\sum_{l=0}^4 c_l |l\rangle_1 \otimes |0\rangle_2$ of the two qubits becomes

$$(c_0 |0\rangle_1 + c_2 |2\rangle_1 + c_3 |3\rangle_1 + c_4 |4\rangle_1) |0\rangle_2 - c_1 |0\rangle_1 |1\rangle_2. \quad (2)$$

Equation (2) shows that the population of the level $|1\rangle$ of qudit 1 is transferred onto the level $|1\rangle$ of qudit 2 [Fig. 2(b)].

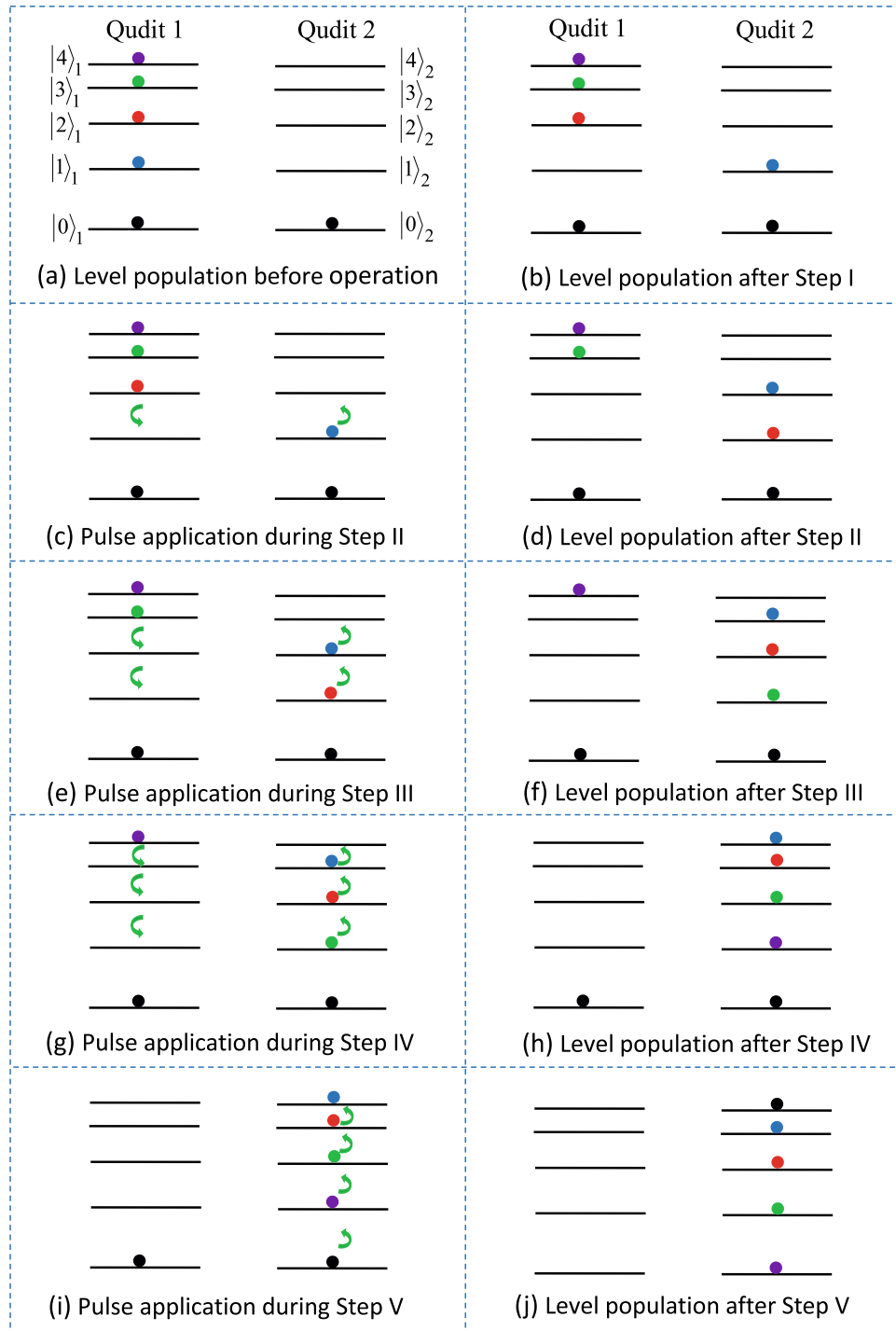


Figure 2. The color circles indicate the occupied energy levels. Each green arrow represents a classical pulse, which is resonant with the transition between the two neighbor levels close to each green arrow. In (e) and (g), the sequence for applying the pulses is from top to bottom, and the lower pulses are turned on after the upper pulses are switched off. In (i), the sequence for applying the pulses is from bottom to top, and the upper pulses are turned on after the lower pulses are switched off. For the details on the applied pulses, see the descriptions given in the text. Note that in (a–j), the left levels are for qudit 1 while the right levels are for qudit 2. For simplicity, we here consider the case that the spacings between adjacent levels become narrow as the levels move up, which is actually unnecessary.

Step II. Apply a pulse of $\{\pi/2, \pi/2\Omega, \omega_{12}\}$ to qudit 1 while a pulse of $\{-\pi/2, \pi/2\Omega, \omega_{12}\}$ to qudit 2 [Fig. 2(c)]. According to Eq. (17), the pulses lead to $|2\rangle_1 \rightarrow |1\rangle_1$ and $|1\rangle_2 \rightarrow |2\rangle_2$. Thus, the state (2) becomes

$$(c_0|0\rangle_1 + c_2|1\rangle_1 + c_3|3\rangle_1 + c_4|4\rangle_1)|0\rangle_2 - c_1|0\rangle_1|2\rangle_2. \quad (3)$$

For $\Omega \gg g$, the interaction between the cavity and the qudits can be neglected during the pulse. Now let the cavity resonant with the $|0\rangle \leftrightarrow |1\rangle$ transition of each qudit for an interaction time $t_2 = \pi/(\sqrt{2}g)$, to obtain the state transformation (1). Hence, the state (3) becomes

$$(c_0|0\rangle_1 + c_3|3\rangle_1 + c_4|4\rangle_1)|0\rangle_2 + (-c_2|1\rangle_2 - c_1|2\rangle_2)|0\rangle_1, \quad (4)$$

which shows that the populations for the levels $|1\rangle$ and $|2\rangle$ of qudit 1 are transferred onto the levels $|2\rangle$ and $|1\rangle$ of qudit 2, respectively [Fig. 2(d)].

Step III. Apply a pulse of $\{\pi/2, \pi/2\Omega, \omega_{23}\}$ and then a pulse of $\{\pi/2, \pi/2\Omega, \omega_{12}\}$ to qudit 1, while a pulse of $\{-\pi/2, \pi/2\Omega, \omega_{23}\}$ and then a pulse of $\{-\pi/2, \pi/2\Omega, \omega_{12}\}$ to qudit 2 [Fig. 2(e)]. The pulses result in the transformations $|3\rangle_1 \rightarrow |1\rangle_1$ (via $|3\rangle_1 \rightarrow |2\rangle_1 \rightarrow |1\rangle_1$), $|2\rangle_2 \rightarrow |3\rangle_2$ and $|1\rangle_2 \rightarrow |2\rangle_2$. Thus, the state (4) becomes

$$(c_0|0\rangle_1 + c_3|1\rangle_1 + c_4|4\rangle_1)|0\rangle_2 + (-c_2|2\rangle_2 - c_1|3\rangle_2)|0\rangle_1. \quad (5)$$

Let the cavity resonant with the $|0\rangle \leftrightarrow |1\rangle$ transition of each qudit for an interaction time $t_3 = \pi/(\sqrt{2}g)$, to achieve the state transformation (1). Thus, the state (5) becomes

$$(c_0|0\rangle_1 + c_4|4\rangle_1)|0\rangle_2 + (-c_3|1\rangle_2 - c_2|2\rangle_2 - c_1|3\rangle_2)|0\rangle_1, \quad (6)$$

which shows that the populations for the levels $|1\rangle$, $|2\rangle$, and $|3\rangle$ of qudit 1 are transferred onto the levels $|3\rangle$, $|2\rangle$, and $|1\rangle$ of qudit 2, respectively [Fig. 2(f)].

Step IV. Apply pulses of $\{\pi/2, \pi/2\Omega, \omega_{34}\}$, $\{\pi/2, \pi/2\Omega, \omega_{23}\}$ and then $\{\pi/2, \pi/2\Omega, \omega_{12}\}$ to qudit 1 while pulses of $\{-\pi/2, \pi/2\Omega, \omega_{34}\}$, $\{-\pi/2, \pi/2\Omega, \omega_{23}\}$ and then $\{-\pi/2, \pi/2\Omega, \omega_{12}\}$ to qudit 2 [Fig. 2(g)], which leads to the transformations $|4\rangle_1 \rightarrow |1\rangle_1$ (via $|4\rangle_1 \rightarrow |3\rangle_1 \rightarrow |2\rangle_1 \rightarrow |1\rangle_1$), $|3\rangle_2 \rightarrow |4\rangle_2$, $|2\rangle_2 \rightarrow |3\rangle_2$ and $|1\rangle_2 \rightarrow |2\rangle_2$. Hence, the state (6) becomes

$$(c_0|0\rangle_1 + c_4|1\rangle_1)|0\rangle_2 + (-c_3|2\rangle_2 - c_2|3\rangle_2 - c_1|4\rangle_2)|0\rangle_1. \quad (7)$$

Let the cavity resonant with the $|0\rangle \leftrightarrow |1\rangle$ transition of each qudit for an interaction time $t_4 = \pi/(\sqrt{2}g)$, to have the state transformation (1). Thus, the state (7) changes

$$(c_0|0\rangle_2 - c_4|1\rangle_2 - c_3|2\rangle_2 - c_2|3\rangle_2 - c_1|4\rangle_2)|0\rangle_1, \quad (8)$$

which shows that the populations for the levels $|1\rangle_1$, $|2\rangle_1$, $|3\rangle_1$, and $|4\rangle_1$ of qudit 1 have been transferred onto the levels $|4\rangle_2$, $|3\rangle_2$, $|2\rangle_2$, and $|1\rangle_2$ of qudit 2, respectively [Fig. 2(h)]. After this step of operation, to maintain the state (8), the level spacings of the qudits need to be adjusted so that the qudits are decoupled from the cavity.

Step V. By sequentially applying pulses of $\{-\pi/2, \pi/2\Omega, \omega_{01}\}$, $\{-\pi/2, \pi/2\Omega, \omega_{12}\}$, $\{-\pi/2, \pi/2\Omega, \omega_{23}\}$, and then $\{-\pi/2, \pi/2\Omega, \omega_{34}\}$ to qudit 2 [Fig. 2(i)], we obtain the state transformations $|0\rangle_2 \rightarrow |4\rangle_2$ (via $|0\rangle_2 \rightarrow |1\rangle_2 \rightarrow |2\rangle_2 \rightarrow |3\rangle_2 \rightarrow |4\rangle_2$), $|1\rangle_2 \rightarrow -|0\rangle_2$, $|2\rangle_2 \rightarrow -|1\rangle_2$, $|3\rangle_2 \rightarrow -|2\rangle_2$, and $|4\rangle_2 \rightarrow -|3\rangle_2$. Hence, the state (8) becomes

$$(c_4|0\rangle_2 + c_3|1\rangle_2 + c_2|2\rangle_2 + c_1|3\rangle_2 + c_0|4\rangle_2)|0\rangle_1. \quad (9)$$

The result (9) shows that an arbitrary quantum state $\sum_{i=0}^4 c_i|i\rangle_1$ of qudit 1 has been transferred onto qudit 2 via the population transfer from the five levels $\{|0\rangle_1, |1\rangle_1, |2\rangle_1, |3\rangle_1, |4\rangle_1\}$ of qudit 1 to the five levels $\{|4\rangle_2, |3\rangle_2, |2\rangle_2, |1\rangle_2, |0\rangle_2\}$ of qudit 2, respectively [Fig. 2(j)].

Case for $d=4$ and $d=3$. From the above description, it can be found that by performing the operations of steps I, II, and III above, and then by sequentially applying pulses of $\{-\pi/2, \pi/2\Omega, \omega_{01}\}$, $\{-\pi/2, \pi/2\Omega, \omega_{12}\}$, and $\{-\pi/2, \pi/2\Omega, \omega_{23}\}$ to qudit 2, we can obtain the state transformation $\sum_{i=0}^3 c_i|i\rangle_1 \otimes |0\rangle_2 \rightarrow |0\rangle_1 \otimes (c_0|3\rangle_2 + c_1|2\rangle_2 + c_2|1\rangle_2 + c_3|0\rangle_2)$, which implies that the QST for $d=4$ is implemented, i.e., an arbitrary quantum state of qudit 1 is transferred onto qudit 2 via the population transfer from the four levels $\{|0\rangle_1, |1\rangle_1, |2\rangle_1, |3\rangle_1\}$ of qudit 1 to the four levels $\{|3\rangle_2, |2\rangle_2, |1\rangle_2, |0\rangle_2\}$ of qudit 2, respectively.

By performing the operations of steps I and II above, followed by applying pulses of $\{-\pi/2, \pi/2\Omega, \omega_{01}\}$ and then $\{-\pi/2, \pi/2\Omega, \omega_{12}\}$ to qudit 2, the state transformation $\sum_{i=0}^2 c_i|i\rangle_1 \otimes |0\rangle_2 \rightarrow |0\rangle_1 \otimes (c_0|2\rangle_2 + c_1|1\rangle_2 + c_2|0\rangle_2)$ can be achieved, which shows that the QST for $d=3$ (i.e., the QST between two qutrits) is realized, i.e., an arbitrary quantum state of qudit 1 is transferred onto qudit 2 via transferring the populations of the three levels $\{|0\rangle_1, |1\rangle_1, |2\rangle_1\}$ of qudit 1 to the three levels $\{|2\rangle_2, |1\rangle_2, |0\rangle_2\}$ of qudit 2, respectively.

Case for any positive integer d . By examining the operations introduced in subsection A (i.e., QST for $d=5$), one can easily find that an arbitrary d -dimensional quantum state can be transferred between two d -level qudits for any positive integer d , through the following d operational steps. The first operational step is the same as that described in step 1 above. For the l^{th} operational step ($1 < l < d$), $l-1$ pulses of $\{\pi/2, \pi/2\Omega, \omega_{(l-1)l}\}, \dots, \{\pi/2, \pi/2\Omega, \omega_{23}\}$, and $\{\pi/2, \pi/2\Omega, \omega_{12}\}$ should be applied to qudit 1 in turn (from left to right), while other $l-1$ pulses of $\{-\pi/2, \pi/2\Omega, \omega_{(l-1)l}\}, \dots, \{-\pi/2, \pi/2\Omega, \omega_{23}\}$, and $\{-\pi/2, \pi/2\Omega, \omega_{12}\}$ should be applied to qudit 2 in sequence (from left to right), followed by each qudit simultaneously resonantly interacting with the cavity for an interaction

time $t = \pi/(\sqrt{2}g)$. One can easily check that after the first $d - 1$ steps of operation, the following state transformation can be obtained $\sum_{l=0}^{d-1} c_l |l\rangle_1 \otimes |0\rangle_2 \rightarrow |0\rangle_1 \otimes (c_0 |0\rangle_2 - \sum_{l=1}^{d-1} c_l |d - l\rangle_2)$, which can further turn into

$$\sum_{l=0}^{d-1} c_l |l\rangle_1 \otimes |0\rangle_2 \rightarrow |0\rangle_1 \otimes (c_0 |d - 1\rangle_2 + c_1 |d - 2\rangle_2 + \dots + c_{d-1} |0\rangle_2), \tag{10}$$

by sequentially applying pulses of $\{-\pi/2, \pi/2\Omega, \omega_{01}\}, \{-\pi/2, \pi/2\Omega, \omega_{12}\}, \dots$, and then $\{-\pi/2, \pi/2\Omega, \omega_{(d-2)(d-1)}\}$ to qudit 2 (i.e., the last step of operation). The result (10) implies that an arbitrary d -dimensional quantum state of qudit 1 (known or unknown) has been transferred onto qudit 2 through the population transfer from the d levels $\{|0\rangle_1, |1\rangle_1, |2\rangle_1, \dots, |d - 2\rangle_1, |d - 1\rangle_1\}$ of qudit 1 to the d levels $\{|d - 1\rangle_2, |d - 2\rangle_2, \dots, |2\rangle_2, |1\rangle_2, |0\rangle_2\}$ of qudit 2, respectively.

Possible experimental implementation. For an experimental implementation, let us now consider a setup of two superconducting transmon qudits embedded in a 3D cavity. This architecture is feasible in the state-of-the-art superconducting setup as demonstrated recently in ref. 11. For simplicity, we consider QST between the two transmon qudits 1 and 2 for $d \leq 5$. As an example, suppose that the state of qudit 1 to be transferred is: (i) $\frac{1}{\sqrt{3}} \sum_{l=0}^2 |l\rangle_1$ for $d=3$, (ii) $\frac{1}{2} \sum_{l=0}^3 |l\rangle_1$ for $d=4$, and (iii) $\frac{1}{\sqrt{5}} \sum_{l=0}^4 |l\rangle_1$ for $d=5$.

We take into account the influence of the unwanted coupling of the cavity with the $|1\rangle \leftrightarrow |2\rangle$ transition. The Hamiltonian $H_{I,1}$ is thus modified as

$$H'_{I,1} = H_{I,1} + \varepsilon_1, \tag{11}$$

where ε_1 describes the unwanted off-resonant coupling between the cavity and the $|1\rangle \leftrightarrow |2\rangle$ transition of each qudit, which is given by $\varepsilon_1 = \sum_{j=1}^2 \tilde{g}_j [a\sigma_{12,j}^+ e^{i(\omega_{12}-\omega_c)t} + h.c.]$ where \tilde{g}_j is the coupling constant between the cavity and the $|1\rangle \leftrightarrow |2\rangle$ transition of qudit j ($j=1, 2$), ω_c is the frequency of the cavity and $\sigma_{12,j}^+ = |2\rangle_j \langle 1|$. For a transmon qudit, one has $\tilde{g}_j \sim \sqrt{2}g_j$ ⁶³.

We also consider the effect of the unwanted couplings of the pulse with the two adjacent $|l - 2\rangle \leftrightarrow |l - 1\rangle$ and $|l\rangle \leftrightarrow |l + 1\rangle$ transitions, when the pulse is resonant with the $|l - 1\rangle \leftrightarrow |l\rangle$ transition of each qudit. Here and below, $l \in \{1, 2, 3, 4\}$ for $d=5$, $l \in \{1, 2, 3\}$ for $d=4$, and $l \in \{1, 2\}$ for $d=3$. After this consideration, the Hamiltonian $H_{I,l}$ is modified as

$$H'_{I,l} = H_{I,l} + H'_{I,1} + \varepsilon_l, \tag{12}$$

where ε_l describes the unwanted off-resonant couplings of the pulse with the $|l - 2\rangle \leftrightarrow |l - 1\rangle$ and $|l\rangle \leftrightarrow |l + 1\rangle$ transitions of each qudit, during the pulse resonant with the $|l - 1\rangle \leftrightarrow |l\rangle$ transition of each qudit [i.e., the pulse frequency is equal to $\omega_{(l-1)l}$]. Here, ε_l is given by

$(\Omega/\sqrt{2})\{e^{-i\varphi} e^{-i[\omega_{(l-1)l} - \omega_{(l-2)(l-1)}]t} |l - 2\rangle \langle l - 1| + h.c.\} + \sqrt{2}\Omega\{e^{i\varphi} e^{i[\omega_{(l-1)l} - \omega_{(l+1)l}]t} |l\rangle \langle l + 1| + h.c.\}$ ⁶³. Note that the effect of the cavity-qudit interaction during the pulse application is also considered here, which is described by the $H'_{I,1}$.

For a transmon qudit, the transition between non-adjacent levels is forbidden or very weak⁶³. Thus, the couplings of the cavity/pulses with the transitions between non-adjacent levels can be neglected. In addition, the spacings between adjacent levels for a transmon qudit become narrow as the levels move up (Fig. 2). Therefore, the detunings between the cavity frequency and the transition frequencies for adjacent levels (e.g., levels $|1\rangle$ and $|2\rangle$, levels $|2\rangle$ and $|3\rangle$, levels $|3\rangle$ and $|4\rangle$, etc.) increase when the levels go up. As a result, when compared with the coupling effect of the cavity with the $|1\rangle \leftrightarrow |2\rangle$ transition, the coupling effect of the cavity with the transitions for other adjacent levels is negligibly small, which is thus not considered in the numerical simulation for simplicity. For similar reasons, when the pulse is resonant with the $|l - 1\rangle \leftrightarrow |l\rangle$ transition of each qudit, the coupling effect of the pulses with the transitions between other adjacent levels is weak and thus we only consider the effect of the coupling of the pulse with the two adjacent $|l - 2\rangle \leftrightarrow |l - 1\rangle$ and $|l\rangle \leftrightarrow |l + 1\rangle$ transitions.

When the dissipation and dephasing are included, the dynamics of the lossy system is determined by the following master equation

$$\begin{aligned} \frac{d\rho}{dt} = & -i[H', \rho] + \kappa \mathcal{L}[a] \\ & + \sum_{j=1}^2 \sum_{l=1}^{d-1} \{\gamma_{(l-1)l,j} \mathcal{L}[\sigma_{(l-1)l,j}^-]\} \\ & + \sum_{j=1}^2 \sum_{l=1}^{d-1} \{\gamma_{\varphi l,j} (\sigma_{ll,j} \rho \sigma_{ll,j} - \sigma_{ll,j} \rho / 2 - \rho \sigma_{ll,j} / 2)\}, \end{aligned} \tag{13}$$

where $d \in \{3, 4, 5\}$, H' is the modified Hamiltonian $H'_{I,1}$ or $H'_{I,l}$ given above, $\sigma_{(l-1)l,j}^- = |l - 1\rangle_j \langle l|$, $\sigma_{ll,j} = |l\rangle_j \langle l|$, and $\mathcal{L}[\Lambda] = \Lambda \rho \Lambda^\dagger - \Lambda^\dagger \Lambda \rho / 2 - \rho \Lambda^\dagger \Lambda / 2$ with $\Lambda = a$, $\sigma_{(l-1)l,j}^-$. Here, κ is the photon decay rate of the cavity. In addition, $\gamma_{(l-1)l,j}$ is the energy relaxation rate of the level $|l\rangle$ for the decay path $|l\rangle \rightarrow |l - 1\rangle$ and $\gamma_{\varphi l,j}$ is the dephasing rate of the level $|l\rangle$ of qudit j ($j=1, 2$).

The fidelity of the operation is given by $\mathcal{F} = \sqrt{\langle \psi_{id} | \rho | \psi_{id} \rangle}$, where $|\psi_{id}\rangle$ is the output state of an ideal system (i.e., without dissipation and dephasing considered), which is given by: (i) $|\psi_{id}\rangle = |0\rangle_1 |0\rangle_c \otimes (1/\sqrt{3}) \sum_{l=0}^2 |l\rangle_2$ for $d=3$,

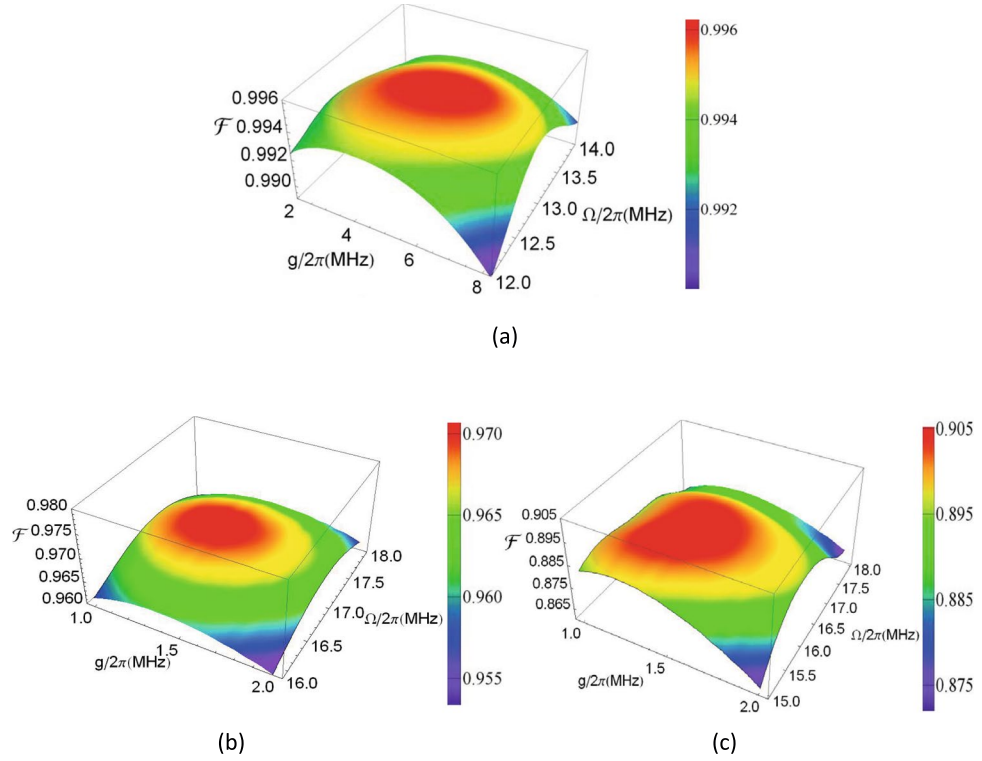


Figure 3. Fidelity for the quantum state transfer for $g/2\pi$ and $\Omega/2\pi$. **(a)** Fidelity for $d=3$. **(b)** Fidelity for $d=4$. **(c)** Fidelity for $d=5$.

(ii) $|\psi_{id}\rangle = |0\rangle_1|0\rangle_c \otimes (1/2)\sum_{l=0}^3|l\rangle_2$ for $d=4$, and (iii) $|\psi_{id}\rangle = |0\rangle_1|0\rangle_c \otimes (1/\sqrt{5})\sum_{l=0}^4|l\rangle_2$ for $d=5$. Note that ρ is the final density operator of the system when the operation is performed in a realistic situation.

Without loss of generality, consider identical transmon qutrits. In this case, the decoherence rates are the same for each qutrit and thus the subscript j involved in the decoherence rates above can be omitted. According to ref. 11, we choose $\omega_{01}/2\pi = 4.97$ GHz, $(\omega_{01} - \omega_{12})/2\pi = 275$ MHz, $(\omega_{12} - \omega_{23})/2\pi = 309$ MHz, and $(\omega_{23} - \omega_{34})/2\pi = 358$ MHz. The decoherence times for the qutrits and the cavity, used in the numerical calculation, are as follows: $\gamma_{01}^{-1} = 84$ μ s, $\gamma_{12}^{-1} = 41$ μ s, $\gamma_{23}^{-1} = 30$ μ s, $\gamma_{34}^{-1} = 22$ μ s, $\gamma_{\varphi 1}^{-1} = 72$ μ s, $\gamma_{\varphi 2}^{-1} = 32$ μ s, $\gamma_{\varphi 3}^{-1} = 12$ μ s, $\gamma_{\varphi 4}^{-1} = 2$ μ s, and $\kappa^{-1} = 15$ μ s. The decoherence times of transmon qutrits considered here are realistic because they are from the recent experimental report in ref. 11. In a realistic situation, it may be a challenge to obtain exact identical qutrit-resonator couplings. Therefore, we consider inhomogeneous qutrit-resonator couplings, e.g., $g_1 = g$ and $g_2 = 0.95g$.

We numerically calculate the fidelity of the entire operation based on the master equation. Figure 3(a,b,c) shows the fidelity versus $g/2\pi$ and $\Omega/2\pi$ for QST between two qutrits for $d=3$, $d=4$, and $d=5$, respectively. From Fig. 3(a), one can see that for $g/2\pi \in [2, 8]$ MHz and $\Omega/2\pi \in [12, 14]$ MHz, the fidelity can be greater than 98.8% for $d=3$. When $g/2\pi = 5.4$ MHz and $\Omega/2\pi = 12.8$ MHz, the fidelity value is the optimum with a value of $\sim 99.6\%$ for $d=3$. As shown in Fig. 3(b), the value of the fidelity has a slow decline for $d=4$. In Fig. 3(b) the optimal value for $\mathcal{F} \sim 96.96\%$ is obtained for $g/2\pi = 1.35$ MHz and for $\Omega/2\pi = 17.00$ MHz. While \mathcal{F} drastically decreases for $d=5$, a high fidelity $\sim 90.32\%$ is attainable with $g/2\pi = 1.45$ MHz and $\Omega/2\pi = 16.00$ MHz [see Fig. 3(c)]. Note that the above values of the g and Ω are readily available in experiments^{64–67}.

To investigate the effect of the pulse errors on the fidelity of the QST, we consider a small frequency error $A\omega$, a small phase error $B\phi$, and a small duration error Ct of each pulse. The frequency, initial phase, and duration $\{\omega, \phi, t\}$ of the pulses are thus modified as $\{\omega + A\omega, \phi + B\phi, t + Ct\}$, where the ω, ϕ, ϕ , and t can be found for each of the pulses applied during the QST, as described in Section Results. With this modification, we numerically calculate the fidelity and plot Fig. 4, which shows how the fidelity of the QST varies with parameters A, B , and C . The values of g and Ω used in Fig. 4 are the ones just mentioned above, corresponding to the optimum fidelities in Fig. 3 for $d=3$, $d=4$, and $d=5$, respectively. Other parameters used in the numerical simulation for Fig. 4 are the same as those used in Fig. 3. Figure 4(a) shows that the effect of the pulse frequency error on the fidelity is negligibly small for $A \in [-10^{-4}, 10^{-4}]$, which corresponds to the pulse frequency error $A\omega \in [-10^{-4}\omega, 10^{-4}\omega]$. Figure 4(b) shows that for $d=3$ and $d=4$, the fidelity is almost unaffected by the pulse phase error for $B \in [-2 \times 10^{-2}, 2 \times 10^{-2}]$; and for $d=5$ the fidelity has a small decrease for $B \in [-5 \times 10^{-2}, 2 \times 10^{-2}]$. Figure 4(c) shows that the effect of the pulse duration error on the fidelity is negligible for $C \in [-2 \times 10^{-2}, 2 \times 10^{-2}]$ for $d=3$, $d=4$ and $C \in [-5 \times 10^{-2}, 2 \times 10^{-2}]$ for $d=5$. These results indicate that compared to the phase error and the duration error, the fidelity is more sensitive to the pulse frequency error. From Fig. 4, one can see that the QST with high fidelity can be achieved for small errors in pulse frequency, phase, and duration.

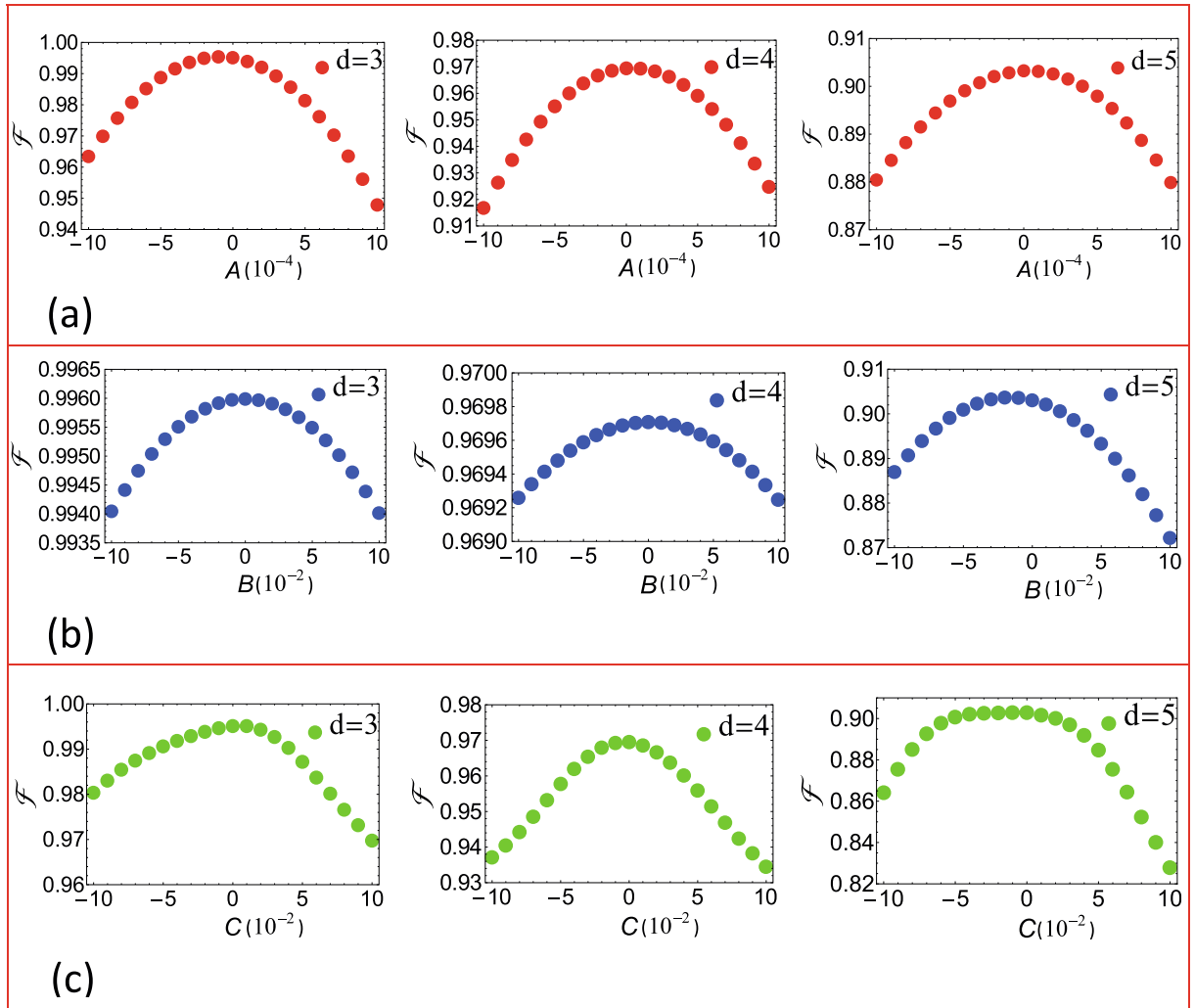


Figure 4. Fidelity versus A , B , and C for $d=3$, $d=4$, and $d=5$, respectively. (a) Fidelity versus A . (b) Fidelity versus B . (c) Fidelity versus C .

For a cavity with frequency $\omega_c/2\pi = 4.97$ GHz and dissipation time κ^{-1} used in the numerical simulation, the quality factor of the cavity is $Q \sim 4.7 \times 10^5$. Note that three-dimensional cavities with a loaded quality factor $Q > 10^6$ have been implemented in experiments^{64,68}.

Discussion

We have presented a method to deterministically transfer arbitrary d -dimensional quantum states (known or unknown) between two superconducting transmon qubits, which are coupled to a single cavity or resonator. As shown above, only a single cavity or resonator is needed, thus the experimental setup is very simple and the inter-cavity crosstalk is avoided. The state transfer can be performed by employing resonant interactions only. In addition, no measurement is required. Numerical simulation shows that high-fidelity transfer of quantum states between two transmon qubits for ($d \leq 5$) is feasible with current circuit-QED technology. This proposal can be extended to transfer an arbitrary d -dimension quantum state between “ladder-type level structure” natural atoms (e.g., Rydberg atoms) or other artificial atoms (e.g., superconducting Xmon qubits, phase qubits, quantum dots), by employing a single cavity only.

The number of pulses can be reduced at a cost of using more than one cavity coupled to the qubits. However, the QST experimental setup will become complicated and the inter-cavity crosstalk is an issue, if two or more cavities are employed instead of a single cavity. Realistic QIP may not involve a large d . To the best of our knowledge, none of experimental works on QIP with qubits of $d > 3$ has been reported. In this sense, we think that this work is of interest. We hope this work will stimulate experimental activities in the near future.

Methods

Hamiltonian and time evolution. Consider two qubits 1 and 2 coupled by a cavity. The cavity is resonant with the transition between the two levels $|0\rangle$ and $|1\rangle$ of each qubit. In the interaction picture, the Hamiltonian is given by (in units of $\hbar = 1$)

$$H_{I,1} = \sum_{j=1}^2 g_j (a\sigma_{0,1,j}^+ + h.c.), \quad (14)$$

where a is the photon annihilation operator for the cavity, the subscript j represents qudit j , $\sigma_{0,1,j}^+ = |1\rangle_j \langle 0|$, and g_j is the coupling constant between the cavity and the $|0\rangle \leftrightarrow |1\rangle$ transition of qudit j ($j = 1, 2$). For simplicity, we set $g_1 = g_2 \equiv g$, which can be achieved by a prior design of qudits or adjusting the position of each qudit located at the cavity.

Under the Hamiltonian (14), one can obtain the following state evolutions:

$$\begin{aligned} |0\rangle_1 |0\rangle_c |0\rangle_2 &\rightarrow |0\rangle_1 |0\rangle_c |0\rangle_2, \\ |1\rangle_1 |0\rangle_c |0\rangle_2 &\rightarrow \frac{1}{2}(1 + \cos\sqrt{2}gt)|1\rangle_1 |0\rangle_c |0\rangle_2 \\ &\quad - \frac{\sqrt{2}}{2}i \sin(\sqrt{2}gt)|0\rangle_1 |1\rangle_c |0\rangle_2 \\ &\quad - \frac{1}{2}(1 - \cos\sqrt{2}gt)|0\rangle_1 |0\rangle_c |1\rangle_2, \end{aligned} \quad (15)$$

where $|0\rangle_c$ ($|1\rangle_c$) represents the vacuum (single photon) state of the cavity and subscript 1 (2) represents qudit 1 (2).

We now consider applying a classical pulse to a qudit, which is resonant with the transition between the level $|l-1\rangle$ and the higher-energy level $|l\rangle$ of the qudit ($l = 1, 2, \dots, d-1$). The Hamiltonian in the interaction picture is expressed as

$$H_{I,l} = \Omega(e^{i\phi}|l-1\rangle\langle l| + h.c.), \quad (16)$$

where Ω and ϕ are the Rabi frequency and the initial phase of the pulse. One can obtain the following rotations under the Hamiltonian (16),

$$\begin{aligned} |l-1\rangle &\rightarrow \cos(\Omega t)|l-1\rangle - ie^{-i\phi} \sin(\Omega t)|l\rangle, \\ |l\rangle &\rightarrow \cos(\Omega t)|l\rangle - ie^{i\phi} \sin(\Omega t)|l-1\rangle. \end{aligned} \quad (17)$$

The results given in Eqs (15) and (17) will be employed for implementing QST between two qudits, which is described in the Section Results.

References

- Muthukrishnan, A. & Stroud, C. R. Multivalued logic gates for quantum computation. *Phys. Rev. A* **62**, 052309 (2000).
- Bullock, S. S., O'Leary, D. P. & Brennen, G. K. Asymptotically optimal quantum circuits for d -level systems. *Phys. Rev. Lett.* **94**, 230502 (2005).
- Bruß, D. & Macchiavello, C. Optimal eavesdropping in cryptography with three-dimensional quantum states. *Phys. Rev. Lett.* **88**, 127901 (2002).
- Cerf, N. J., Bourennane, M., Karlsson, A. & Gisin, N. Security of quantum key distribution using d -level systems. *Phys. Rev. Lett.* **88**, 127902 (2002).
- Dada, A. C., Leach, J., Buller, G. S., Padgett, M. J. & Andersson, E. Experimental high-dimensional two-photon entanglement and violations of generalized Bell inequalities. *Nat. Physics* **7**, 677–680 (2011).
- Kiktenko, E. O., Fedorov, A. K., Man'ko, O. V. & Man'ko, V. I. Multilevel superconducting circuits as two-qubit systems: Operations, state preparation, and entropic inequalities. *Phys. Rev. A* **91**, 042312 (2015).
- Kiktenko, E. O., Fedorov, A. K., Strakhov, A. A. & Man'ko, V. I. Single qudit realization of the Deutsch algorithm using superconducting many-level quantum circuits. *Phys. Lett. A* **379**, 1409–1413 (2015).
- Lanyon, B. P. *et al.* Simplifying quantum logic using higher-dimensional Hilbert spaces. *Nat. Physics* **5**, 134–140 (2009).
- Chow, J. M. *et al.* Microwave-activated conditional-phase gate for superconducting qubits. *New J. Phys.* **15**, 115012 (2013).
- Neeley, M. *et al.* Emulation of a quantum spin with a superconducting phase qudit. *Science* **325**, 722–725 (2009).
- Peterer, M. J. *et al.* Coherence and decay of higher energy levels of a superconducting transmon qubit. *Phys. Rev. Lett.* **114**, 010501 (2015).
- Kumar, K. S., Vepsäläinen, A., Danilin, S. & Paraoanu, G. S. Stimulated Raman adiabatic passage in a three-level superconducting circuit. *Nat. Commun.* **7**, 10628 (2016).
- Clarke, J. & Wilhelm, F. K. Superconducting quantum bits. *Nature* **453**, 1031–1042 (2008).
- You, J. Q. & Nori, F. Atomic physics and quantum optics using superconducting circuits. *Nature* **474**, 589–597 (2011).
- Buluta, I., Ashhab, S. & Nori, F. Natural and artificial atoms for quantum computation. *Rep. Prog. Phys.* **74**, 104401 (2011).
- Chow, J. K. *et al.* Universal quantum gate set approaching fault-tolerant thresholds with superconducting qubits. *Phys. Rev. Lett.* **109**, 060501 (2012).
- Chang, J. B. *et al.* Improved superconducting qubit coherence using titanium nitride. *Appl. Phys. Lett.* **103**, 012602 (2013).
- Barends, R. *et al.* Coherent Josephson qubit suitable for scalable quantum integrated circuits. *Phys. Rev. Lett.* **111**, 080502 (2013).
- Chow, J. M. *et al.* Implementing a strand of a scalable fault-tolerant quantum computing fabric. *Nature Comm.* **5**, 4015 (2014).
- Chen, Y. *et al.* Qubit architecture with high coherence and fast tunable coupling. *Phys. Rev. Lett.* **113**, 220502 (2014).
- Stern, M. *et al.* Flux qubits with long coherence times for hybrid quantum circuits. *Phys. Rev. Lett.* **113**, 123601 (2014).
- Neeley, M. *et al.* Process tomography of quantum memory in a Josephson-phase qubit coupled to a two-level state. *Nat. Physics* **4**, 523–526 (2008).
- Leek, P. J. *et al.* Using sideband transitions for two-qubit operations in superconducting circuits. *Phys. Rev. B* **79**, 180511 (2009).
- Strand, J. D. *et al.* First-order sideband transitions with flux-driven asymmetric transmon qubits. *Phys. Rev. B* **87**, 220505 (2013).
- Blais, A., Huang, R. S., Wallraff, A., Girvin, S. M. & Schoelkopf, R. J. Cavity quantum electrodynamics for superconducting electrical circuits: an architecture for quantum computation. *Phys. Rev. A* **69**, 062360 (2004).

26. Yang, C. P., Chu, S. I. & Han, S. Possible realization of entanglement, logical gates, and quantum-information transfer with superconducting-quantum-interference-device qubits in cavity QED. *Phys. Rev. A* **67**, 042311 (2003).
27. You, J. Q. & Nori, F. Quantum information processing with superconducting qubits in a microwave field. *Phys. Rev. B* **68**, 064509 (2003).
28. Wallraff, A. *et al.* Strong coupling of a single photon to a superconducting qubit using circuit quantum electrodynamics. *Nature* **431**, 162–167 (2004).
29. Chiorescu, I. *et al.* Coherent dynamics of a flux qubit coupled to a harmonic oscillator. *Nature* **431**, 159–162 (2004).
30. Forn-Daz, P. *et al.* Observation of the Bloch-Siegert shift in a qubit-oscillator system in the ultrastrong coupling regime. *Phys. Rev. Lett.* **105**, 237001 (2010).
31. Niemczyk, T. *et al.* Circuit quantum electrodynamics in the ultrastrong-coupling regime. *Nat. Physics* **6**, 772–776 (2010).
32. Blais, A., van den Brink, A. M. & Zagoskin, A. M. Tunable coupling of superconducting qubits. *Phys. Rev. Lett.* **90**, 127901 (2003).
33. Plastina, F. & Falci, G. Communicating Josephson qubits. *Phys. Rev. B* **67**, 224514 (2003).
34. Yang, C. P. & Han, S. *n*-qubit-controlled phase gate with superconducting quantum-interference devices coupled to a resonator. *Phys. Rev. A* **72**, 032311 (2005).
35. Helmer, F. & Marquardt, F. Measurement-based synthesis of multiqubit entangled states in superconducting cavity QED. *Phys. Rev. A* **79**, 052328 (2009).
36. Bishop, L. S. *et al.* Proposal for generating and detecting multi-qubit GHZ states in circuit QED. *New J. Phys.* **11**, 073040 (2009).
37. Yang, C. P., Liu, Y. X. & Nori, F. Phase gate of one qubit simultaneously controlling *n* qubits in a cavity. *Phys. Rev. A* **81**, 062323 (2010).
38. DiCarlo, L. *et al.* Demonstration of two-qubit algorithms with a superconducting quantum processor. *Nature* **460**, 240–244 (2009).
39. Chow, J. M. *et al.* Simple all-microwave entangling gate for fixed-frequency superconducting qubits. *Phys. Rev. Lett.* **107**, 080502 (2011).
40. Mariani, M. *et al.* Implementing the quantum von Neumann Architecture with superconducting circuits. *Science* **334**, 61–65 (2011).
41. Fedorov, A., Steffen, L., Baur, M., da Silva, M. P. & Wallraff, A. Implementation of a Toffoli gate with superconducting circuits. *Nature* **481**, 170–172 (2012).
42. Reed, M. D. *et al.* Realization of three-qubit quantum error correction with superconducting circuits. *Nature* **482**, 382–385 (2012).
43. DiCarlo, L. *et al.* Preparation and measurement of three-qubit entanglement in a superconducting circuit. *Nature* **467**, 574–578 (2010).
44. Novikov, S. *et al.* Raman coherence in a circuit quantum electrodynamics lambda system. *Nat. Physics* **12**, 75–79 (2016).
45. Averin, D. V. *et al.* Suppression of dephasing by qubit motion in superconducting circuits. *Phys. Rev. Lett.* **116**, 010501 (2016).
46. Yang, C. P., Chu, S. I. & Han, S. Quantum information transfer and entanglement with SQUID qubits in cavity QED: A Dark-state scheme with tolerance for nonuniform device parameter. *Phys. Rev. Lett.* **92**, 117902 (2004).
47. Kis, Z. & Paspalakis, E. Arbitrary rotation and entanglement of flux SQUID qubits. *Phys. Rev. B* **69**, 024510 (2004).
48. Paspalakis, E. & Kylstra, N. J. Coherent manipulation of superconducting quantum interference devices with adiabatic passage. *J. Mod. Opt.* **51**, 1679–1689 (2004).
49. Yang, C. P. Quantum information transfer with superconducting flux qubits coupled to a resonator. *Phys. Rev. A* **82**, 054303 (2010).
50. Feng, Z. B. Quantum state transfer between hybrid qubits in a circuit QED. *Phys. Rev. A* **85**, 014302 (2012).
51. Yang, C. P., Su, Q. P. & Nori, F. Entanglement generation and quantum information transfer between spatially-separated qubits in different cavities. *New J. Phys.* **15**, 1150031 (2013).
52. Majer, J. *et al.* Coupling superconducting qubits via a cavity bus. *Nature* **449**, 443–447 (2007).
53. Sillanpää, M. A., Park, J. I. & Simmonds, R. W. Coherent quantum state storage and transfer between two phase qubits via a resonant cavity. *Nature* **449**, 438–442 (2007).
54. Baur, M. *et al.* Benchmarking a quantum teleportation protocol in superconducting circuits using tomography and an entanglement witness. *Phys. Rev. Lett.* **108**, 040502 (2012).
55. Steffen, L. *et al.* Deterministic quantum teleportation with feed-forward in a solid state system. *Nature* **500**, 319–322 (2013).
56. Qin, W., Wang, C. & Long, G. L. High-dimensional quantum state transfer through a quantum spin chain. *Phys. Rev. A* **87**, 012339 (2013).
57. Liu, Y. & Zhou, D. L. Transfer of an arbitrary photon state along a cavity array without initialization. *New J. Phys.* **17**, 013032 (2015).
58. Bayat, A. & Karimipour, V. Transfer of *d*-level quantum states through spin chains by random swapping. *Phys. Rev. A* **75**, 022321 (2007).
59. Bayat, A. Arbitrary perfect state transfer in *d*-level spin chains. *Phys. Rev. A* **89**, 062302 (2014).
60. Ghosh, J. Emulating quantum state transfer through a spin-1 chain on a one-dimensional lattice of superconducting qubits. *Phys. Rev. A* **90**, 062318 (2014).
61. Liu, T., Xiong, S. J., Cao, X. Z., Su, Q. P. & Yang, C. P. Efficient transfer of an arbitrary qutrit state in circuit quantum electrodynamics. *Opt. Lett.* **40**, 5602–5605 (2015).
62. Yang, C. P., Su, Q. P., Zheng, S. B. & Nori, F. Crosstalk-insensitive method for simultaneously coupling multiple pairs of resonators. *Phys. Rev. A* **93**, 042307 (2016).
63. Koch, J. *et al.* Charge-insensitive qubit design derived from the Cooper pair box. *Phys. Rev. A* **76**, 042319 (2007).
64. Paik, H. *et al.* Observation of high coherence in Josephson junction qubits measured in a three-dimensional circuit QED architecture. *Phys. Rev. Lett.* **107**, 240501 (2011).
65. Rigetti, C. *et al.* Superconducting qubit in a waveguide cavity with a coherence time approaching 0.1 ms. *Phys. Rev. B* **86**, 100506 (2012).
66. Baur, M. *et al.* Measurement of Autler-Townes and mollow transitions in a strongly driven superconducting qubit. *Phys. Rev. Lett.* **102**, 243602 (2009).
67. Yoshihara, F. *et al.* Flux qubit noise spectroscopy using Rabi oscillations under strong driving conditions. *Phys. Rev. B* **89**, 020503 (2014).
68. Reagor, M. *et al.* Quantum memory with millisecond coherence in circuit QED. *Phys. Rev. B* **94**, 014506 (2016).

Acknowledgements

C.P. Yang and Q.P. Su were supported in part by the Ministry of Science and Technology of China under Grant No. 2016YFA0301802, the National Natural Science Foundation of China under Grant Nos 11074062, 11504075, and 11374083, and the Zhejiang Natural Science Foundation under Grant No. LZ13A040002. J.M. Liu was supported in part by the National Natural Science Foundation of China under Grant Nos 11174081 and 11134003, the National Basic Research Program of China under Grant No. 2012CB821302, and the Natural Science Foundation of Shanghai under Grant No. 16ZR1448300. This work was also supported by the funds from Hangzhou City for the Hangzhou-City Quantum Information and Quantum Optics Innovation Research Team.

Author Contributions

T.L. and C.P.Y. conceived the idea. T.L. carried out all calculations under the guidance of Q.P.S. and C.P.Y. T.L., Q.P.S., J.H.Y., Y.Z., S.J.X., J.M.L., and C.P.Y. discussed the results. T.L., Q.P.S., and C.P.Y. contributed to the writing of the manuscript.

Additional Information

Competing Interests: The authors declare that they have no competing interests.

Publisher's note: Springer Nature remains neutral with regard to jurisdictional claims in published maps and institutional affiliations.



Open Access This article is licensed under a Creative Commons Attribution 4.0 International License, which permits use, sharing, adaptation, distribution and reproduction in any medium or format, as long as you give appropriate credit to the original author(s) and the source, provide a link to the Creative Commons license, and indicate if changes were made. The images or other third party material in this article are included in the article's Creative Commons license, unless indicated otherwise in a credit line to the material. If material is not included in the article's Creative Commons license and your intended use is not permitted by statutory regulation or exceeds the permitted use, you will need to obtain permission directly from the copyright holder. To view a copy of this license, visit <http://creativecommons.org/licenses/by/4.0/>.

© The Author(s) 2017